1-1-2014

Effect of austenite deformation temperature on Nb clustering and precipitation in microalloyed steel

E V Pereloma
University of Wollongong, elenap@uow.edu.au

A G Kostryzhev
University of Wollongong, andrii@uow.edu.au

A Alshahrani
The University of Wollongong, amfa065@uowmail.edu.au

C Zhu
The University of Sydney, czhu@uow.edu.au

J M. Cairney
The University of Sydney

See next page for additional authors

Effect of austenite deformation temperature on Nb clustering and precipitation in microalloyed steel

Abstract

The effect of thermomechanical processing conditions on Nb clustering and precipitation in both austenite and ferrite in a Nb-Ti microalloyed steel was studied using electron microscopy and atom probe tomography. A decrease in the deformation temperature increased the Nb-rich precipitation in austenite and decreased the extent of precipitation in ferrite. Microstructural mechanisms that explain this variation are discussed.

Keywords

precipitation, clustering, nb, temperature, steel, deformation, microalloyed, austenite, effect

Disciplines

Engineering | Science and Technology Studies

Publication Details

Pereloma, E., Kostryzhev, A., Alshahrani, A., Zhu, C., Cairney, J. M., Killmore, C. R. & Ringer, S. P. (2014). Effect of austenite deformation temperature on Nb clustering and precipitation in microalloyed steel. Scripta Materialia, 75 (March), 74-77.

Authors

E V Pereloma, A G Kostryzhev, A Alshahrani, C Zhu, J M. Cairney, C R. Killmore, and S P. Ringer

Effect of Austenite Deformation Temperature on Nb Clustering and Precipitation in Microalloyed Steel

E.V. Pereloma[a,b], A.G. Kostryzhev[a*], A. AlShahrani[a], C. Zhu[c,d],
J. M. Cairney[c,d], C. R. Killmore[e] and S.P. Ringer[c,d]
[a]School of Mechanical, Materials and Mechatronic Engineering, University of Wollongong, NSW 2522, Australia;
[b]UOW Electron Microscopy Centre, University of Wollongong, NSW 2519, Australia;
[c]Australian Centre for Microscopy and Microanalysis, The University of Sydney, NSW 2006, Australia;
[d]School of Aerospace, Mechanical and Mechatronic Engineering, The University of Sydney, NSW 2006, Australia;
[e]BlueScope Steel Ltd., Five Islands Rd, Port Kembla, NSW 2500, Australia
*corresponding author e-mail: andrii@uow.edu.au

Abstract
The effect of thermo-mechanical processing conditions on Nb clustering and precipitation in both austenite and ferrite in a Nb-Ti microalloyed steel was studied using electron microscopy and atom probe tomography. A decrease in the deformation temperature increased the Nb-rich precipitation in austenite and decreased the extent of precipitation in ferrite. Microstructural mechanisms that explain this variation are discussed.

Key words: Nb clustering, precipitation, steel, atom probe tomography, electron microscopy

The wide range of mechanical properties attainable in high strength low alloy (HSLA) steels coupled with their relatively low cost are responsible for their high volume of production, which represents approximately 10 % of the world's steel production. The high yield strengths of these steels (~ 550 - 600 MPa) arise through microalloying (< 0.1 wt. %) of Nb, Ti and V. A vast amount of research [1-2] has been directed to understanding of the mechanisms by which these microalloying elements modify the steel microstructure, and thereby influence the mechanical properties. At high temperatures, the microstructure of these steels is affected by the processes of recovery, recrystallisation and grain boundary-particle interactions [1-5]. The microalloying elements retard austenite recrystallisation via solute drag and/or particle pinning of grain boundaries, and this leads to austenite grain refinement. At low temperatures in ferrite, dislocation-particle interactions lead to precipitation strengthening [6]. One of the most protracted debates amongst researchers for the last 30 years has been the relative role of microalloyed solute atoms versus the role of strain-induced precipitation on the kinetics of austenite recrystallisation. Much of this debate has been in the area of Nb-bearing HSLA steels [7]. Some authors consider that solute atoms are more effective in retarding recrystallisation [4,8], while others argue that precipitates are more effective [9,10]. To obtain the desired overall microstructure requires a tuning of the grain size, dislocation sub-structure and precipitate dispersions, and this in turn requires that some of the thermo-mechanical processing (TMP) is conducted above and below the recrystallisation temperature. In this work, we compare and contrast the distribution of Nb in a HSLA steel subjected to deformation in these two temperature regions. This analysis was carried out using atom probe tomography (APT), which is proven to be an effective technique to provide information about the precise 3D arrangement of the Nb atoms in the form of segregation, clustering and precipitation in steels [11,12].

A microalloyed steel produced by the BlueScope Steel Ltd. containing 0.081C-1.20Mn-0.27Si-0.021Ni-0.019Cr-0.1Mo-0.016Cu-0.037Al-0.064Nb-0.021Ti-0.003V-0.001S-0.012P-0.0047N (wt. %) was subjected to TMP using a Gleeble 3500 simulator [13]. The steel was firstly austenitised at 1250 °C for 300 s, and then given a roughing deformation strain of 0.35 at a strain rate of 5 s^{-1} at 1100 °C. The samples were then cooled at 1 °Cs^{-1} to either 1075 or 825 °C, and

deformed up to a strain of 0.75 at a strain rate of 5 s^{-1}. After this, three cooling schedules were employed: (1) a water quench, (ii) cooling at 1 °Cs^{-1} to 800 °C (above the austenite-to-ferrite transformation start temperature), followed by a water quench at ~160 °Cs^{-1}, and (iii) cooling at 1 °Cs^{-1} to 600 °C (in the ferrite temperature region), holding for 300 s, followed by air cooling to room temperature. As the microstructures formed on quenching were mainly martensitic with some lower bainite, it is assumed that no redistribution of substitutional elements has taken place. Thus, our use of APT provided insight into the distribution of alloying elements in austenite before the quench. Tips for atom probe were prepared from the centre of the Gleeble samples perpendicular to the compression axis following a standard two-stage electropolishing procedure [14, 15]. Atom probe data was collected on a Cameca Local Electrode Atom Probe (LEAP™), operating at a temperature of 20 K and a pulse fraction rate of 20%. The data reconstruction was performed following the methodology described in [16]. Solute atom clustering and fine precipitation were identified and analysed using a maximum distance separation program provided by Dr M.K. Miller, Oak Ridge National Laboratory, USA. The Guinier radii, r_G, of clusters/fine carbides were calculated from radii of gyration (l_g) data using the equation, $r_G = \sqrt{(5/3)}\, l_g$ [14,15]. The determined cluster size takes into account the 57% detection efficiency and is based on the positions of all detected atoms. Thin foils for transmission electron microscopy (TEM) studies were prepared using tripod polishing method and ion milling. FEGTEM observations were carried out on a JEOL JEM-2200FS, using an accelerating voltage of 200 kV. Statistical analysis of precipitation was undertaken on JEOL 7001F FEG scanning electron microscope (SEM) operating at 5 kV, which allowed analysis of particles down to 20 nm size.

A summary of precipitate number density distributions in samples studied using SEM is given in Fig. 1. As both series of samples were subjected to the same austenitising and roughing conditions, the distributions of coarse > 70 nm TiN and (Ti,Nb)(C,N) particles are similar, and therefore are not a point for discussion here. On cooling below 1100 °C, which was estimated to be the dissolution temperature of NbC [17], the formation of precipitates was expected. This process can be accelerated by deformation [18], as crystal defects (dislocation nodes and tangles) provide additional heterogeneous nucleation sites for precipitation. However, 1075 °C was too high a deformation temperature to result in strain-induced precipitation. On the contrary, after deformation at 825 °C the strain-induced precipitation occurred. Analysis of particle number density distributions is consistent with this (Fig. 1). After deformation at 1075 °C the number of < 70 nm particles did not vary significantly during cooling to 800 °C in the austenite temperature region (Fig. 1, a), which indicates absence of strain-induced precipitation. After deformation at 825 °C the number density of < 70 nm particles increased from 0.38 μm^{-2} to 0.93 μm^{-2}, i.e. by 2.4 times, during cooling in austenite (Fig. 1, b), which indicates strain-induced precipitation. In addition, the particle area fraction in the samples quenched from 800 °C was about 50 % higher for the 825 °C TMP schedule compared to that for the 1075 °C schedule ($3.1x10^{-3}$ vs $1.8x10^{-3}$). This precipitation behaviour should have resulted in a larger amount of Nb retained in the austenite solution for the 1075 °C TMP schedule compared to that for the 825 °C schedule, which would lead to a variation in ferrite precipitation. Thus, during holding in ferrite after deformation at 1075 °C the number density of < 70 nm particles increased from 0.36 μm^{-2} (at 800 °C) to 1.44 μm^{-2} (at 600 °C), i.e. by 4 times. During holding in ferrite after deformation at 825 °C the number density of < 70 nm particles increased from 0.93 μm^{-2} (at 800 °C) to 1.15 μm^{-2} (at 600 °C), i.e. by only 24 %. The particle area fraction in the samples deformed at 825 °C increased in ferrite by only $0.1x10^{-3}$ (with respect to the 800 °C quenched condition) reaching $3.2x10^{-3}$, while in the samples deformed at 1075 °C it more than doubled (with respect to the 800 °C quenched condition) reaching $4.7x10^{-3}$. These indicate a much more pronounced particle precipitation in ferrite following deformation at 1075 °C, compared to that at 825 °C. Analysis of the orientation relationships between the NbC and the ferrite matrix for all the TMP schedules revealed (Fig. 2) that some fine precipitates exhibited the Baker-Nutting orientation relationship

(001)NbC//(001)α, [010]NbC//[110]α [19], which indicates they precipitated in ferrite, whereas others did not show these orientations (Fig. 2b) confirming their origin in austenite.

Table 1 shows information about clusters of atoms measured using atom probe, which is able to resolve finer features than the SEM and TEM studies. After deformation at 1075 °C the Nb-C clusters were not observed, with only 2-8 Nb atom clusters being present [13]. On the contrary, after deformation at 825 °C a relatively high number density of Nb-C clusters precipitated (Table 1). This could be a result of both longer cooling time after roughing to 825 °C, compared to that to 1075 °C, and a higher dislocation density after a lower deformation temperature (825 °C vs 1075 °C), which led to an increase in the number of nucleation sites for clusters. After cooling in austenite to 800 °C the Nb-C cluster number density was 5 times higher following deformation at 825 °C, compared to that following deformation at 1075 °C (Table 1, Fig. 3 a,b), which indicates a much higher clustering rate in austenite for the lower deformation temperature schedule. As a result of an increased clustering and precipitation in austenite a matrix depletion in Nb might be expected following deformation at 825 °C, which would lead to the retardation of precipitation in ferrite for this condition. Thus, after holding at 600 °C the number density and cluster size of Nb-C clusters increased from the 1075-800 to 1075-600 TMP condition (Table 1, Fig.3 c) and decreased from the 825-800 to 825-600 TMP condition (Table 1, Fig. 3 d). A larger amount of smaller clusters was observed for the 1075-600 TMP condition, compared to that for the 825-600 TMP condition (Fig. 3, e and f). These indicate a higher clustering rate in ferrite following deformation at a higher temperature and, together with the analysis of particle behaviour (Fig. 1), growth of previously-formed clusters following deformation at a lower temperature. All of the observed clusters were significantly enriched in C (Table 1), which indicates faster clustering of C atoms, probably on pre-existing Nb atom clusters [13], corresponding to a higher rate of diffusion of C atoms in austenite compared to Nb. However, there is 20 to 40% overestimation of C concentration in fine clusters due to the deficiency of the envelope method [20]. During clustering in ferrite the Nb content in clusters increased following deformation at 1075 °C, but did not vary significantly for the samples deformed at 825 °C, which could indicate a higher Nb clustering rate in ferrite due to a higher Nb content remaining in the matrix after a higher deformation temperature. The composition of some coarser clusters approached stoichiometric one (50/50) for the NbC particles. It is possible that these clusters serve as the pre-cursor for NbC particles.

In summary, the study of Nb clustering and precipitation in a microalloyed steel has shown that a decrease in deformation temperature in austenite increases the rate of clustering and precipitation in austenite as a result of slow dislocation annihilation rate and an increased number of cluster/precipitate nucleation sites. Conversely, the precipitation and clustering decrease in ferrite, following the matrix depletion in Nb. While increased austenite precipitation has desirable effects arising from enhanced retardation of recrystallisation and refined grain size, reduced ferrite precipitation may lead to a decrease in the ferrite strengthening.

Acknowledgement
This work was financially supported by the Australian Research Council (LP110100231).

References

1 Microalloying '95: Proceedings of the international conference “Microalloying ‘95”, 11-14 June 1995, Pittsburgh, PA, USA, Iron and Steel Society Inc, 1995.
2 M. Korchynsky, in Proceedings of Int. Symposium on Steel for Fabricated Structures, 1-4 November 1999, Cincinnati, OH, USA, pp. 139-145.
3 L.Q. Ma, Z.Y. Liu, S.H. Jiao, X.Q. Yuan, D. Wu, J. Iron Steel Res. Int. 15 (2008) 31-36.
4 C.L. Miao, C.J. Shang, H.S. Zurob, G.D. Zhang, and S.V. Subramanian, Met. Mat. Trans. A 43 (2012) 665 – 676.

5 B. Dutta, E.J. Palmiere and C. M. Sellars, Acta Mat. 49 (2001) 785 - 794.
6 T. Gladman, The physical metallurgy of microalloyed steels, The Institute of Materials, Cambridge University Press, Cambridge, 1997.
7 A.J. DeArdo, Int. Mater. Rev. 48(6) (2003) 371 - 402.
8 O. Kwon, A.J. DeArdo, Acta Metall. Mater. 39(4) (1991) 529 - 538.
9 S. Vervynckt, K. Verbeken, P. Thibaux, Y. Houbaert, Mat. Sci. Eng. A 528 (2011) 5519 - 5528.
10 C.R. Hutchinson, H.S. Zurob, C.W. Sinclair and Y.J.M. Brechet, Scripta Mat. 59 (2008) 635 - 637.
11 E.V. Pereloma, I.B. Timokhina, K. Russell and M. Miller, Scripta Mat. 54 (2006) 471-476.
12 Y. Xie, T.X. Zheng, J.M. Cairney, H. Kaul, J.G. Williams, C.C. Killmore, S.P. Ringer, Scripta Mat. 66 (2012) 710-713.
13 A. G. Kostryzhev, A. AlShahrani, C. Zhu, S. P. Ringer, E. V. Pereloma, Mat. Sci. Eng. A 581 (2013) 16-25.
14 B.G. Gault, M.P. Moody, J.M. Cairney, S.P. Ringer, Atom Probe Microscopy, Springer, New York, 2012.
15 M.K. Miller, Atom Probe Tomography: Analysis at the Atomic Level, Springer, New York, 2000.
16 M.P. Moody, B. Gault, L.T. Stephenson, D. Haley, S.P. Ringer, Ultramicroscopy 109 (2009) 815 - 824.
17 B. Soenen, S. Jacobs and C. Klinkenberg, Proc. Materials Solutions Conf., (2002) 7 - 9 October, Columbus, Ohio, USA, pp. 16 – 24.
18 B. Dutta and C. M. Sellars, Mater. Sci. Tech. 3, (1987) 197-206
19 R. G. Baker and J. Nutting, Precipitation Processes in Steel, Special Report 64, Iron and Steel Institute, London, 1959.
20 E.V. Pereloma, M.K. Miller, I.B. Timokhina, Met. Mat. Trans. A, 39A (2008) 3210-3216.

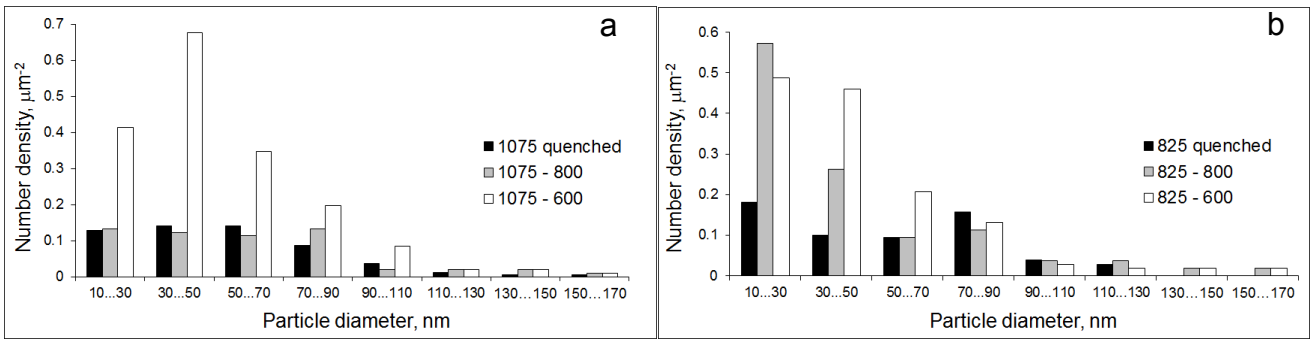

Fig. 1 Nb-rich precipitate number density distributions after various cooling schedules for samples deformed at (a) 1075 °C and (b) 825 °C.

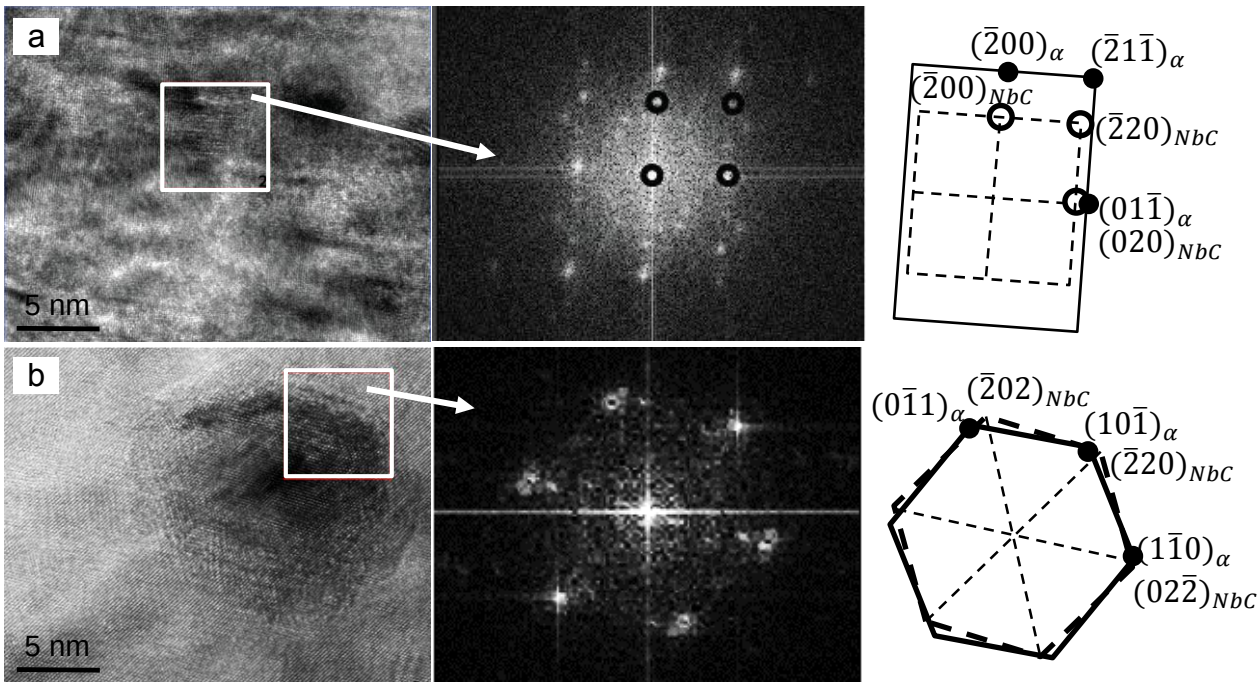

Fig. 2 Representative HRTEM images and corresponding diffraction patterns of NbC (a) with Baker-Nutting orientation relationship and (b) without orientation relationship to ferrite.

Table 1 Characterisation of C-Nb clusters/fine precipitates after different TMP schedules

TMP condition	C, at %	Nb, at %	Fe, at %	r_G, nm	Cluster size, number of atoms	Number density, $x10^5$ μm^{-3}
1075-800	84.4 ± 8.7	8.1 ± 5.1	5.3 ± 4.3	1.7 ± 0.2	20-31	0.12
1075-600	70.0 ± 6.0	23 ± 5.0	6.6 ± 2.2	2.8 ± 1.3	20-580	0.6
825	83.2 ±7.2	15.7 ± 7	1.1 ± 1.1	2.3 ± 0.2	23-28	0.4
825-800	67.5 ± 7.2	27.8 ± 7	4.6 ± 2.4	2.3 ± 1.1	20-758	0.6
825-600	66.8 ± 5.4	24.6 ± 5	8.0 ± 2.6	2.8 ± 1	20-601	0.34

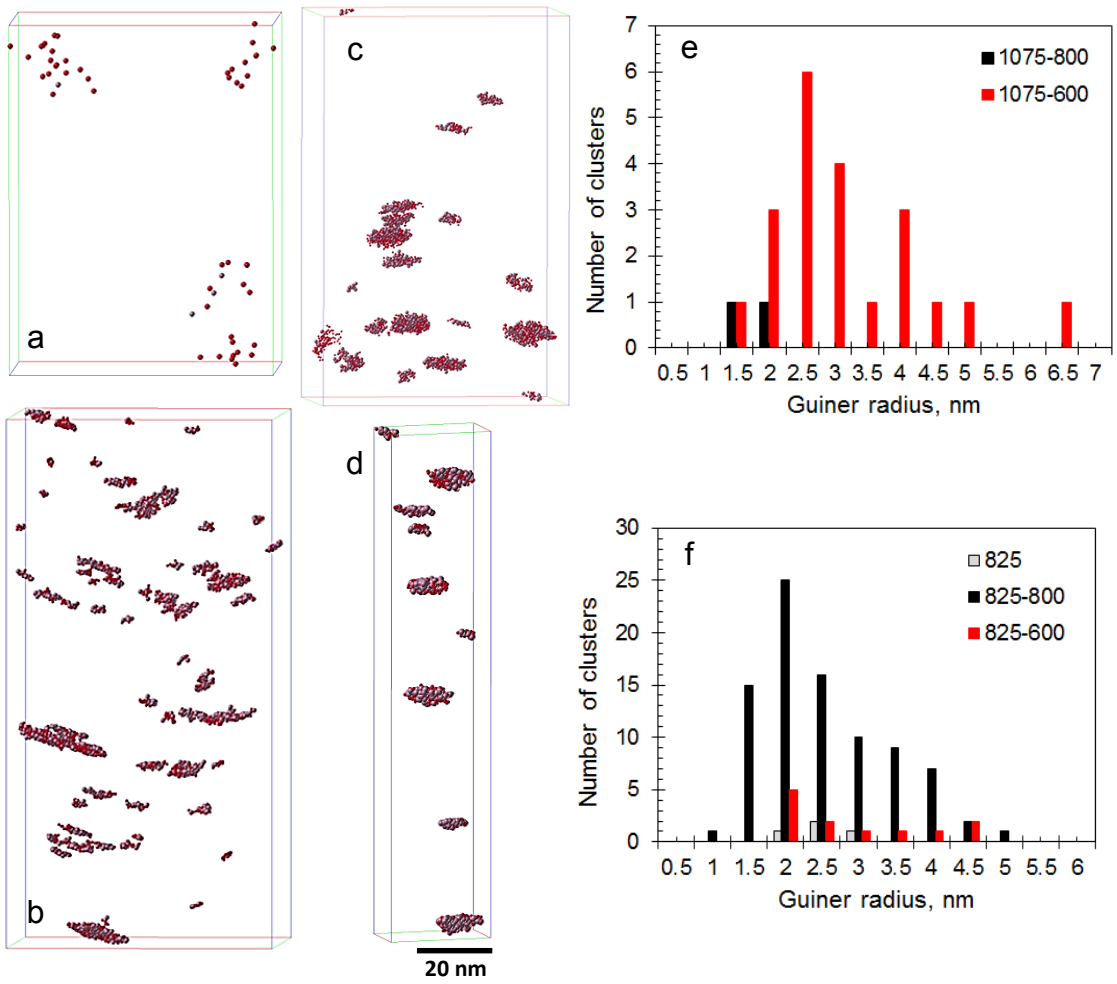

Fig. 3 Selected APT maps showing Nb-C clusters after quenching from 800 °C following deformation at (a) 1075 °C and (b) 825 °C, and after holding at 600 °C following deformation at (c) 1075 °C and (d) 825 °C; (e) and (f) are cluster size distributions for 1075 and 825 °C deformation temperature TMP schedules.